Journal of Building Engineering 50 (2022) 104081

Contents lists available at ScienceDirect

Journal of Building Engineering

journal homepage: www.elsevier.com/locate/jobe

Consolidation of clay-rich earthen building materials: A comparative study at the Alhambra fortress (Spain)

Kerstin Elert [a,*], Fadwa Jroundi [b], Cristina Benavides-Reyes [c], Elena Correa Gómez [d], Davide Gulotta [e], Carlos Rodriguez-Navarro [a]

[a] University of Granada, Dept. of Mineralogy and Petrology, Fuentenueva S/N, 18071 Granada, Spain
[b] University of Granada, Dept. of Microbiology, Fuentenueva S/N, 18071 Granada, Spain
[c] University of Granada, Dept. of Operative Dentistry, Campus de Cartuja, 18071 Granada, Spain
[d] Conservation Department, Council of the Alhambra and Generalife, 18009 Granada, Spain
[e] Getty Conservation Institute, Los Angeles, USA

ARTICLE INFO

Keywords:
Rammed earth
Ethyl silicate
Nanolime
Nanosilica
Alkaline activation
Bacterial biomineralization

ABSTRACT

Earth has been an important construction material throughout history. Being a relatively fragile material, it can undergo extensive weathering depending on prevailing climate conditions, consequently requiring constant maintenance and often consolidation. The latter is still one of the most challenging tasks in the conservation field. Here we compare the effectiveness of a conventional consolidant (ethyl silicate) with several more recently introduced consolidants (nanolime and nanosilica) and consolidation methods (alkaline activation and bacterial biomineralization). Improvements in weathering resistance, water drop absorption, contact angle, and water vapor transmission, as well as mechanical strength (drilling resistance and compressive strength) of laboratory-prepared rammed earth mock-ups and a rammed earth wall at the Alhambra (Granada, Spain) were evaluated and related to treatment-induced compositional and textural changes. A detailed analysis of advantages and shortcomings of each consolidant was performed and modifications to current application protocols are proposed to optimize the efficacy of conventional and novel consolidation treatments.

1. Introduction

The consolidation of earthen architecture is one of the most challenging tasks in the conservation field and over the years many different treatment methods and products have been proposed to address the conservation needs of historic earthen buildings and archaeological remains [1–5]. Important architectural heritage made of rammed earth or adobe can be found in most parts of the world and more recently earth has experienced a revival in the search for sustainable building materials for new constructions [6]. Depending on the prevailing climatic conditions, the maintenance requirements of earthen structures vary, but might be substantial if they are exposed to important seasonal precipitation. Consequently, consolidation treatments (i.e., application of a strengthening/cementing agent to the substrate in order to regain lost cohesion of the degraded surface [7]) are often necessary in order to prolong the structure's service life and reduce maintenance. However, as compared to other building materials such as lime mortars or stone, the number of systematic studies on the effectiveness of consolidation treatments for earthen structures is limited.

Past organic and inorganic consolidants have not always offered satisfactory results over the long run. Indeed, consolidation of

* Corresponding author.
E-mail address: kelert@ugr.es (K. Elert).

https://doi.org/10.1016/j.jobe.2022.104081
Received 15 December 2021; Received in revised form 17 January 2022; Accepted 17 January 2022
Available online 29 January 2022

earthen structures is especially challenging considering the material's intrinsic characteristics, namely the often significant content in clay minerals. Clay acts as a binder for coarser soil fractions including sand and gravel, but, at the same time, can be the cause of degradation (i.e., cracking and material loss) due to its response (i.e. swelling or contraction) to changes in the substrate's moisture content [8]. Repeated volume changes and associated stress can result in the deterioration of the consolidant's effectiveness over time, which has been reported for example in the case of alkoxysilanes, one of the most commonly used consolidants for earthen material [9]. Consequently some researchers have suggested that the main aim of a consolidation treatment for clay-rich substrates should be a reduction in the soil's swelling capacity rather than a simple increase in strength [10]. The consolidation of earthen structures is often further complicated by delamination and the presence of cracks of important depth, which facilitate the penetration of water into unconsolidated interior zones favoring material loss due to scaling or spalling.

Here we compare the effectiveness of a conventional consolidant (i.e., ethyl silicate) with several consolidants (i.e., nanosilica and nanolime) and consolidation methods (i.e., alkaline activation and bacterial biomineralization), which have been more recently proposed for the treatment of earthen structures [2,4,5,11,12]. In the case of ethyl silicate- and nanosilica-based consolidants, the final product is amorphous silica gel, which forms upon solvent evaporation and subsequent hydrolysis and/or polycondensation (i.e., sol-gel process). The silanols formed during hydrolysis of ethyl silicate might not only react with one another upon condensation to form siloxane (Si–O–Si) bonds, but also with OH-groups on the (silicate) mineral surface, thus inducing strong cementation of the substrate [13]. Nanolime contains portlandite ($Ca(OH)_2$) nanoparticles dispersed in alcohol, which carbonate rapidly when in contact with ambient CO_2 and result in a cementation of the treated substrate. Alkaline activation using KOH solution relies on the partial dissolution of soil minerals (i.e., clays and other reactive aluminum-silicate phases) at high pH and the subsequent formation of amorphous zeolitic precursors with cementing properties [2,9]. In addition, KOH and $Ca(OH)_2$ might induce flocculation (i.e.,

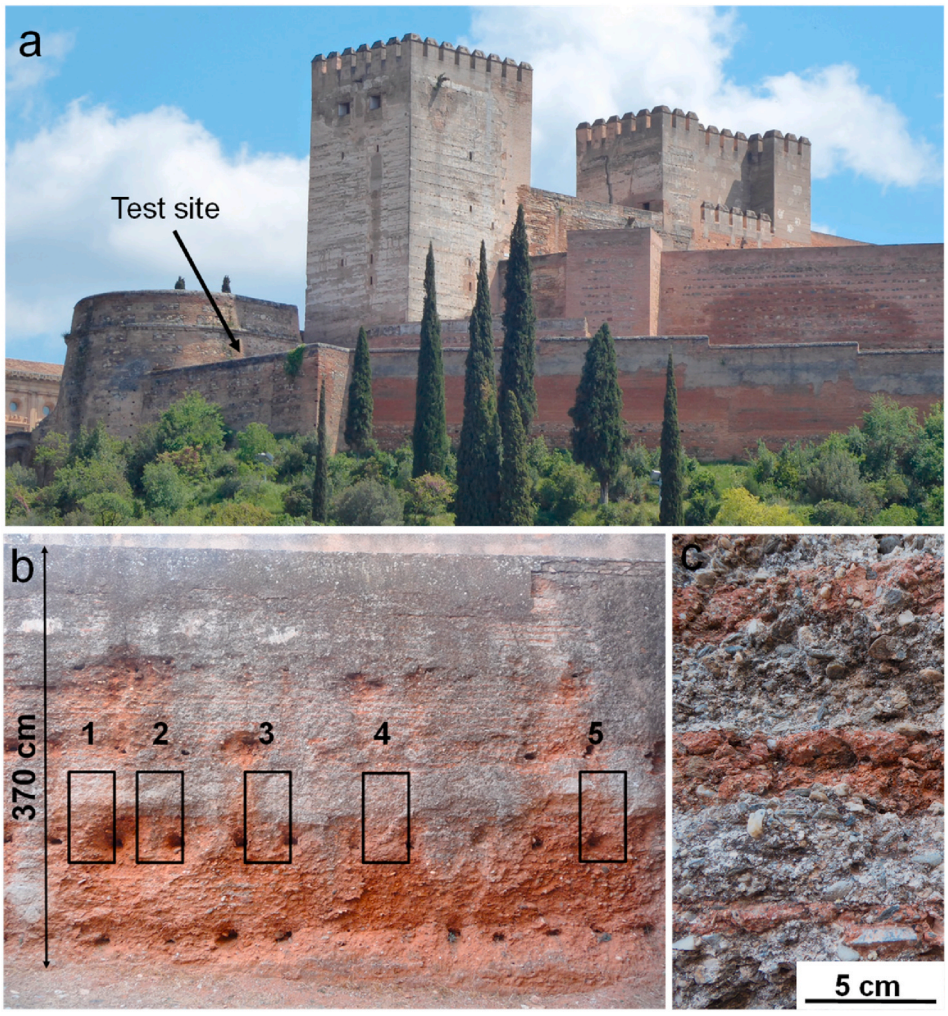

Fig. 1. a) General view of part of the Alhambra Alcazaba (Fortress, Granada, Spain). The arrow indicates the location of the test site; b) XIII century rammed earth wall, showing treatment areas: (1) ethyl silicate, (2) nanolime, (3) nanosilica, (4) alkaline activation (2 M KOH), and (5) bacterial biomineralization; and c) detail of the degraded lime-amended earthen wall, showing alternating grey lime-rich and red clay-rich layers. (For interpretation of the references to color in this figure legend, the reader is referred to the Web version of this article.)

decrease in clay particle repulsion in the presence of an electrolyte) and cation exchange in the case of Na-smectites, thus reducing clay swelling to a certain extent [14,15]. Several bacterial biomineralization strategies exist, which all rely on the precipitation of a cementing hybrid material containing calcium carbonate and bacterially-derived exopolymeric substances (EPS, composed of polysaccharides, proteins, DNA, and RNA) [16]. Previous studies suggest that clay swelling might be controlled by the intercalation of bacterial EPS into the interlayer space of expansive clays [17]. Exogenous or stone isolated single bacterial cultures have commonly been applied for biomineralization treatments [18]. However, more recently a simplified method, which involves the application of a patented sterile nutritive solution (i.e., source of Ca and amino acids) to selectively activate the carbonatogenic bacteria among the indigenous microbial community, has been developed [19,20]. This method eliminates the need for the isolation and culture of a carbonatogenic bacteria inoculum in the laboratory prior to application. So far it has been successfully applied to limestone, tuff, and gypsum plaster, but its effectiveness for the consolidation of earthen architectural heritage has not been explored [16,21,22].

The evaluation of each consolidant included its penetration and cementation capacity (i.e., strength increase), as well as possible improvements in the weathering resistance of earthen structures. The results obtained here were related to changes in mineralogical composition, texture, surface properties (water contact angle) and porosity, induced by the consolidants applied under laboratory conditions (i.e., rammed earth mock-ups) and *in situ* (i.e., rammed earth wall, XIII century) at the Alhambra Fortress, which is the most important example of Nasrid architecture in southern Spain (Fig. 1). The outcome of our research illustrates the advantages and shortcomings of each consolidant in a systematic manner and lays the basis for further advances in the development of more suitable products and treatment methods for the consolidation of earthen structures.

2. Materials and methods

2.1. Rammed earth wall for in situ treatment

For the *in situ* treatment a south-facing rammed earth wall at the Alhambra fortress was selected as a pilot area (Fig. 1). This earthen wall is representative in terms of structure, composition and level of weathering of most original earthen walls present at the Alhambra fortress. It shows different levels of erosion due to granular disintegration (Fig. S1a, Supplementary Information). The upper part is still covered by a lime-rich layer (Fig. 1b), whereas the lower part has suffered severe erosion, displaying in some areas alternating grey lime-rich and reddish clay-rich layers, typical for lime-amended rammed earth constructions (Fig. 1c). In addition, large amounts of pebbles contribute to a significant inhomogeneity of the earthen structure (Fig. S1b, Supplementary Information). The evaluation of the consolidant effectiveness in this study was limited to the reddish clay-rich layers (i.e., those areas displaying the most severe damage and material loss).

2.2. Preparation of rammed earth mock-ups

Considering the historical-cultural value of the earthen structures at the Alhambra fortress, it was not possible to directly collect large samples of the historic rammed earth wall to perform a detailed laboratory study complementing the *in situ* tests. Therefore, it was decided to prepare mock-ups with local earthen material from the Alhambra formation outcrops, which have historically been used for the construction of earthen structures in Granada, including the Alhambra and the city walls [9]. Because the durability of earthen structures is to a great extent determined by the erosion resistance of the soil matrix, the fine soil fraction ($\leq$1 mm, obtained by sieving) was selected for the preparation of mock-ups in order to obtain a homogeneous matrix (i.e., many tests such as peeling test, or drilling resistance and contact angle measurements, are difficult to perform in the presence of pebbles) and facilitate the evaluation of the consolidation effectiveness, in particular with regard to the swelling capacity of clay minerals. Earth mock-ups (4 $\times$ 4x4 cm) were prepared with a water/solid ratio of 0.2 (by weight). Wooden frames (16 $\times$ 12 $\times$ 4 cm) were filled with 2 cm thick layers of the soil mixture and compacted manually. Prior to consolidation treatments, mock-ups were dried under laboratory conditions (20 $\pm$ 5 °C, 40 $\pm$ 5% RH) for 2 months.

2.3. In situ treatments at the Alhambra fortress

For the *in situ* treatment 50 $\times$ 100 cm areas of the rammed earth wall were selected for each consolidant. These areas included clay-rich zones of similar level of erosion, which had lost the lime-rich outer layer (Fig. 1b). Loose debris was removed by brush before treatment. Table 1 summarizes information regarding the different consolidation treatments and curing conditions. The

Table 1
Consolidation treatments and curing during *in situ* application.

Consolidant	Appl. method	No. of appl.	Appl. period (days)	Total amount (L/m^2)
Biomineralization[a]	Spray	5	3	10
Nanolime[b]	Brush	5	1	5
Nanosilica[c]	Brush	3	3	3
Alkaline Activation	Brush	5	3	5
Ethyl silicate[d]	Brush	5	1	3

[a] Patented water-based nutritional solution M − 3P [20].
[b] Calosil E25, 25 g/L in ethanol, ~150 nm particle size (IBZ-Salzchemie GmbH&Co.KG, Germany), diluted with ethanol 1:1 to a total solid content of 12.5 g/L.
[c] NanoEstel, solid content: 30 wt%, colloidal silica dispersed in water, 10–20 nm particle size (C.T.S., Spain) diluted with MilliQ water 1:1 to a total solid content of 15 wt%.
[d] Estel 1000 in white spirit D40, solid content: min. 35 wt% (C.T.S., Spain) used as is.

biomineralization treatment involved the repeated application of the patented M − 3P nutritional solution by spray in order to avoid the contamination of the solution during application (as might occur if applied by brush) [20]. All other treatments were applied by brush in order to minimize the health risk (i.e., inhalation of aerosols) to the operator.

Granada has a Mediterranean climate, with significant diurnal and seasonal changes in *T* and RH, as well as important precipitation during the winter months and dry summers. Treatments were applied in October and *T* and RH (i.e., 20 ± 4 °C and 44 ± 10%, respectively) were recorded during treatment with a datalogger that was placed on the wall surface at a distance of 10 cm from the biomineralization test area. Areas treated with the nutritive M − 3P and the 2 M KOH solutions were covered with opaque plastic film for 7 days to avoid premature drying, as well as to prevent direct light irradiation and possible associated bacterial pigmentation in the case of the biomineralization treatment. Analyses and *in situ* tests were performed 6 months after consolidant application, when the test areas were completely dry.

2.4. Laboratory treatments

Table 2 summarizes information regarding the different treatments using identical consolidants as in the *in situ* test. Note, however, that the amount of consolidant applied to the rammed earth wall was substantially higher than that of the laboratory-treated rammed earth mock-ups (12 specimens per consolidant) as a result of the increased absorption capacity of the former and lower RH during *in situ* treatment application, which enabled faster drying between each application.

Curing of all mock-ups (with the exception of samples treated with ethyl silicate, which were kept at ~50% RH during curing) took place in unsealed plastic boxes to allow for adequate air circulation at ~80% RH (using glass beakers filled with water) in order to facilitate carbonation/alkaline activation and avoid premature drying and/or consolidant backflow upon rapid solvent evaporation. In the case of the biomineralization treatment, daylight was blocked using black plastic film to prevent bacterial-induced pigmentation and consequent color change of the substrate. After curing, all samples were stored under laboratory conditions (20 ± 5 °C, 40 ± 5% RH) for 2 months prior to analysis and testing.

2.5. Analytical methods and testing

Powder X-ray diffraction analysis (XRD, X'Pert PRO, Malvern Panalytical Ltd., UK) was performed to determine the mineralogical composition of laboratory mock-ups and Alhambra rammed earth samples before and after consolidation. Additionally, oriented aggregates of the clay fraction of the 1 mm thick surface layer of earth mock-ups, either air-dried or treated with dimethyl sulfoxide (DMSO), were analyzed. Equipment settings: Cu-Kα radiation; Ni filter; 45 kV voltage; 40 mA intensity; exploration range of 3°–60°2θ and goniometer speed of 0.05°2θ s^{-1}. Mineral phase identification and quantification were performed using HighScore (Malvern Panalytical Ltd., UK) and XPowder software [23] and experimental reference intensity ratio (RIR) values.

Thermogravimetric-differential scanning calorimetry (TGA-DSC) analysis on a Mettler TGA/DSC 3+ Star was used to quantify mineral phases and organic matter before and after bacterial biomineralization of rammed earth samples. Analysis conditions: alumina crucibles, ~40 mg samples mass, 25–950 °C *T*-range, and 100 mL/min gas flow. Samples were analyzed in air and N_2 (i.e., weight loss and an exothermic band are only expected during combustion of organics in air but not in an inert N_2 atmosphere).

Textural and compositional characteristics of carbon-coated samples before and after consolidation in the laboratory and *in situ* were studied using field emission scanning electron microscopy (FESEM, AURIGA, Carl Zeiss, Germany) coupled with energy dispersive spectrometry (EDS, INCA-200, Oxford Instruments, UK). Equipment settings: 10^{-6} Pa vacuum and 3 kV acceleration voltage in secondary electron imaging mode and 20 kV acceleration voltage for microanalysis.

The total number of culturable bacteria (Colony-forming units, CFU/g) was determined before and 4 or 6 months after the biomineralization treatment of mock-ups and the rammed earth wall, respectively. The extraction protocol for culturable bacteria established by Jroundi et al. [16] was followed to determine the total bacterial count. The carbonatogenic capacity of bacterial isolates cultured in M − 3P solid medium was estimated based on $CaCO_3$ production using optical microscopy.

Color parameters of untreated and treated mock-ups and the rammed earth wall were determined with a spectrophotometer (CM-700 d, Konika Minolta, Japan) using the CIE $L^*a^*b^*$ color space (i.e., L^* is luminosity varying from black with a value of 0 to white with a value of 100; a^* varies from $+a^*$ (red) to $-a^*$ (green) and b^* from $+b^*$ (yellow) to $-b^*$ (blue)). Color change was calculated using the following formula: $\Delta E^* = (\Delta L^{*2} + \Delta a^{*2} + \Delta b^{*2})^{1/2}$. Equipment settings were: illuminant D65, 10° viewing angle, 8 mm Ø aperture. Average values are based on 10 measurements per sample type.

Improvements in water resistance were determined by measuring water absorption and weight loss (4 specimens per sample type)

Table 2
Consolidation treatments and curing during laboratory application.

Consolidant	Appl. method	No. of appl./appl. period (days)	Total amount (L/m^2)	Curing *T* (°C), RH (%)	Curing period (days)
Biomineralization	Spray	6 (5)	1.2	25 ± 5, 80 ± 5	14
Nanolime[a]	Brush	5 (1)	0.15	25 ± 5, 80 ± 5	28
Nanosilica[b]	Brush	5 (1)	0.2	25 ± 5, 80 ± 5	28
Alkaline Activation	Brush	5 (5)	0.7	25 ± 5, 80 ± 5	28
Ethyl silicate[c]	Brush	5 (1)	1.5	25 ± 5, 50 ± 5	28

[a] Calosil E25, 25 g/L in ethanol, ~150 nm particle size (IBZ-Salzchemie GmbH&Co.KG, Germany) used as is.
[b] NanoEstel, solid content: 30 wt%, colloidal silica dispersed in water, 10–20 nm particle size (C.T.S., Spain) used as is.
[c] Estel 1000 in white spirit D40, solid content: min. 35 wt% (C.T.S., Spain) used as is.

upon immersion of untreated and treated mock-ups in water for predetermined time intervals. Note that the water absorption rate (wt %/day) could only be determined for ethyl silicate-treated mock-ups according to standard IS3495:1992 [24] as the remaining samples suffered important weight loss upon immersion and weight gain could not be measured in a consistent manner. It might be argued that wetting-drying cycles would have better mimicked natural weathering processes [25]. However, this type of test would have had an even more severe impact on the clay-rich earth mock-ups of this study and likely not have permitted a comparison of the consolidants' effectiveness [26].

To further evaluate the effectiveness of consolidation treatments, the sessile drop method was applied to determine the static contact angle of 4 μL water drops deposited on the mock-up surface before and after consolidation using an OCA 15 EC equipment (DataPhysics Instruments, Germany) following the procedure described in UNE-EN 828 [27]. The same instrument was used to record videos of the water drop absorption and determine changes in absorption kinetics induced by the different consolidation treatments. Average values are based on at least 3 measurements per sample type.

The water vapor transmission rate (WVTR) of cylindrical samples (Ø = 2.5 cm and height = 1 cm) of earth mock-ups was evaluated using a modified version of the procedure described in UNE-EN 15803 [28]. Due to the limited sample size, cylindrical plastic containers (Ø = 2.5 cm and height = 7 cm, filled with 2 mL saturated KNO_3 solution to maintain 93% RH inside the container) were used instead of the standard cuvette. The seal between sample and container was obtained using plasticine covered by Parafilm®. Samples were kept in an environmental chamber at 50% RH. The test was performed in duplicate over a 10-day period.

Total pore volume and pore size distribution of mock-ups and Alhambra rammed earth samples before and after consolidation were determined with mercury intrusion porosimetry (MIP) using an Autopore III 9410 porosimeter (Micromeritics, Norcross, US). This instrument measures pores with 0.003–360 μm diameter. Samples (~1.5 g) were prepared from the 0.5 cm outer surface layer of mock-ups and the rammed earth wall, which were oven-dried for 48 h at 60 °C prior to analysis. MIP analyses of each sample type were performed at least in duplicate.

An Instron 3345 equipment (Instron Co., Canton, US) was used to determine the increase in compressive strength upon consolidation of earth mock-ups using an adapted version of the procedure described in UNE-EN 1015–11 [29]. Prismatic samples (2 × 1x1 cm) were prepared from a 1 cm thick outer surface layer of the mock-ups. A load of 5000 N at 3 mm/min was applied to at least 4 specimens per sample type.

A portable drilling resistance measurement system (DRMS, Sint Technology, Italy) was used to measure the increase in mechanical strength upon consolidation as well as consolidant penetration depth of mock-ups and the rammed earth wall. In the latter case, drilling resistence measurements were performed *in situ*. The drilling parameters were as follows: 5 mm diamond-tip drill bit, 20 mm maximum depth, 20 mm/min penetration rate, and 400 rpm revolution speed. Average values are based on at least 5 measurements.

The "Scotch tape" or peeling test was used to evaluate changes in surface cohesion upon consolidation in the laboratory and *in situ* [30]. For testing 3 × 3.8 cm adhesive tape stripes were used. Reported average values are based on four tests per sample type.

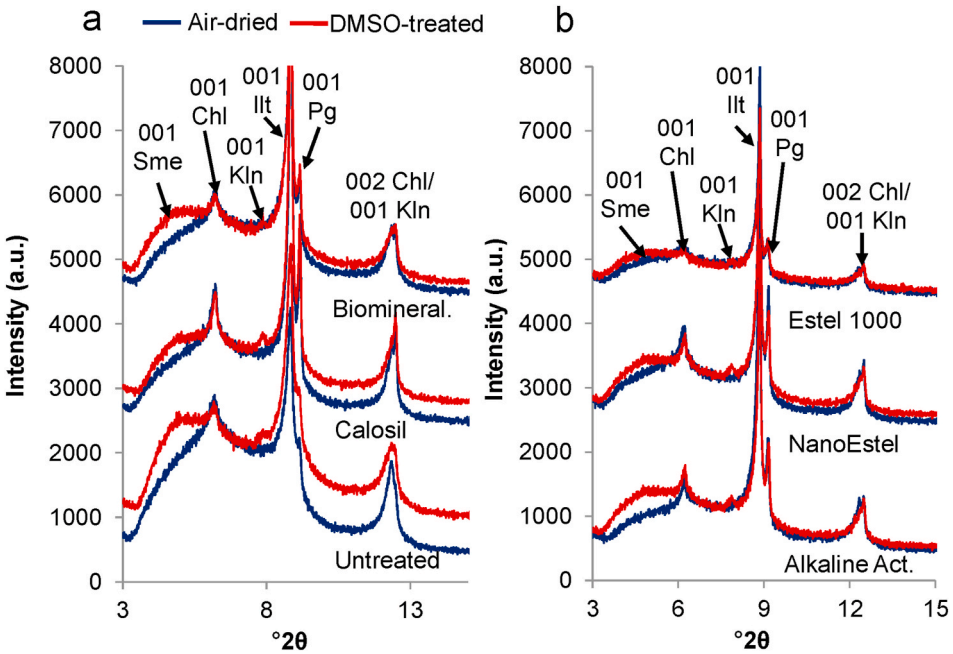

Fig. 2. XRD patterns of air-dried and DMSO-treated oriented aggregates of earth mock-ups (1 mm surface layer) before and after consolidation treatments. Sme = smectite, Chl = chlorite, Kln = kaolinite, Ilt = illite, and Pg = paragonite [33].

3. Results

3.1. Mineralogical composition of mock-ups before and after consolidation

XRD analysis (powder samples) of the Alhambra formation soil used for the preparation of mock-ups revealed a certain inhomogeneity among the different samples with 50–60 wt% clay minerals, 35–40 wt% quartz, and ~5 wt% feldspars. Trace amounts of carbonates and iron-oxihydroxides (i.e., hematite and goethite) were also detected, the latter being responsible for the reddish-brownish color of the soil. The analysis of oriented aggregates allowed the identification of smectite, illite, paragonite, kaolinite and chlorite (Fig. 2). These are, with the exception of paragonite, common clay minerals and typical soil constituents [31]. The presence of expansive clay minerals (i.e., smectites), which can generate pressures of >100 N/mm^2 upon intracrystalline swelling [8], makes this soil especially susceptible to swelling-induced degradation.

After consolidation, a slight increase in calcite was detected in samples treated with nanolime, biomineralization, and alkaline activation. While the formation of calcite is to be expected in the case of the former two treatments, it is rather surprising in the case of the latter, but might be related to the dissolution of Ca-bearing silicate minerals (e.g., smectites) at high pH and subsequent carbonation. The detected amounts of calcite after the biomineralization treatment were comparable to those (i.e., ~2 wt%) detected in archaeological gypsum successfully treated with the same nutritional solution [22]. The remaining consolidation treatments did not provoke any detectable mineralogical changes, which is not surprising considering that they all induce the formation of small amounts of amorphous silica gel or zeolitic precursors difficult to detect and quantify with XRD.

XRD analysis of DMSO-treated oriented aggregates of the 1 mm thick outer surface layer of consolidated earth mock-ups provided important information on the consolidants' effect on the potential swelling capacity of clays. XRD patterns of untreated soil are included for comparison (Fig. 2a). Note that the DMSO treatment not only caused an increase of the d_{001}-spacing of smectites from ~15 Å to ~18 Å, but also affected kaolinite, leading to a shift of the d_{001}-spacing from ~7.15 Å to 11.2 Å [32]. None of the consolidation treatments was able to completely prevent clay swelling, but all led to a certain decrease. In particular, the XRD patterns of the clay fraction of ethyl silicate treated mock-ups showed the smallest changes upon DMSO treatment (i.e., very small left-shift of the low intensity 001 Bragg peak of smectite) (Fig. 2b). Apparently, ethyl silicate cemented clay particles effectively and limited their preferential orientation with the [001] direction normal to the glass slide (i.e., with their (001) planes parallel to the glass slide, Fig. S2, Supplementary Information) as indicated by the intensity increase and broadening of the general Bragg peak of clays at 4.46 Å (indicative of non-oriented clay minerals) and the intensity decrease of the corresponding 00*l* Bragg peaks as compared to the untreated sample. Cementation-induced disorientation of clay particles likely reduces anisotropic (i.e. directional) swelling strain and associated stress. Nonetheless, individual smectite particles can still undergo expansion (Fig. S3, Supplementary Information), suggesting that even in the case of the ethyl silicate-treated earth, limited clay swelling (and subsequently volume changes) can be expected and could degrade its consolidation efficacy over time as has been reported previously [10].

3.2. Mineralogical composition of the Alhambra rammed earth before and after consolidation

In the case of the rammed earth wall (powder samples) of the Alhambra fortress, XRD analyses of the clay-rich red layers showed even larger compositional variations than those observed for the mock-ups, the former containing 15–25 wt% carbonates and 15–25 wt % gypsum additional to 40–50 wt% clay, 15–25 wt% quartz, and ~5 wt% feldspars. The clay mineral composition was similar to that of the earth mock-ups. The relatively high carbonate content is related to the construction technique, implying the presence of remnants of the lime amendment in the clay-rich reddish layers. Regarding the origin of gypsum, it has been reported that gypsum was occasionally used to fill putlog holes of interior rammed earth walls. Its presence is of concern since it is known to accelerate the deterioration of earthen structures [34]. Gypsum could also serve as a sulfate source for the formation of ettringite during the alkaline activation treatment and induce swelling damage [35]. However, ettringite was not detected with XRD or FESEM in any of the samples. Note that apart from the relatively high carbonate and gypsum content, rammed earth samples showed a high degree of similarity with the mock-up samples in terms of silicate mineralogy and contents, confirming that the source of the raw earth material was the same in both cases (i.e., Alhambra formation). Unfortunately, the significant inhomogeneity of the rammed earth wall did not allow the detection of any treatment-related mineralogical changes using XRD. However, TGA/DSC analyses (Fig. S4, Supplementary Information) showed that the $CaCO_3$ content increased from 18 ± 1 wt% before to 24 ± 2 wt% after biomineralization treatment as determined from the weight loss and corresponding endothermic band at 550–850 °C due to the reaction $CaCO_3 = CaO + CO_2$. The value (6 wt%) of newly formed $CaCO_3$ is in good agreement with the amounts of calcite detected in limestone and tuff stone after similar bacterial biomineralization treatment [16,21].

3.3. Bacterial population before and after biomineralization treatment

The total bacterial count revealed that indigenous carbonatogenic bacteria were effectively activated by the biomineralization treatment. The total number of cultured bacteria increased by almost 4 orders of magnitude in earth mock-ups, from $6.59 \pm 1.20 \times 10^3$ CFU/g before treatment to $2.10 \pm 0.04 \times 10^7$ CFU/g after treatment [12]. The total bacteria count in the rammed earth wall at the Alhambra increased from $7.34 \pm 1.37 \times 10^3$ CFU/g before to $2.71 \pm 0.40 \times 10^6$ CFU/g after treatment [12]. The slightly lower increase after the *in situ* treatment is possibly due to less favorable environmental conditions (i.e., nightly temperatures dropped to ~15 °C and the average RH was only ~45%). Optical microscopy observation of bacterial isolates cultured in M − 3P medium proved that all activated bacteria were carbonatogenic and thus capable of inducing the precipitation of calcium carbonate. Note that the values obtained in this study regarding original bacterial count and subsequent increase upon treatment are comparable to those observed for other substrates successfully treated using the same approach, including limestone and tuff [16,21].

3.4. Textural and microstructural features after treatment

FESEM provided important information on the *modus operandi* of the different consolidants. A FESEM image of the unconsolidated rammed earth is included for comparison (Fig. 3a). Microscopic observations revealed the formation of a several micrometer thick layer of aggregated nano-sized calcite particles in the case of the nanolime treatment, regardless of the substrate (i.e., mock-ups or earthen wall at the Alhambra) (Fig. 3b). As the result of an interface-coupled dissolution-precipitation process, the original size of portlandite particles of ~150 nm was maintained upon carbonation [36]. In the case of the biomineralization treatment, FESEM allowed the detection of bacterial fission (Fig. 3c) and the generation of bacterial calcium carbonate (BCC) covered by EPS (Fig. 3d and e), thus offering unambiguous proof of enhanced carbonatogenic bacterial activity and confirming the effectiveness of the bio-treatment *in situ* and in the laboratory [12].

TGA/DSC enabled the quantification of newly formed biomass corresponding to bacterial EPS (plus bacterial cells/debris) in the observed biofilms. The organics content experienced a 3-fold increase from 0.2 wt% before to 0.7 wt% after biomineralization treatment as indicated by the marked exothermic band at 250–450 °C in the DSC curve performed in flowing air (Fig. S4, Supplementary Information).

The nanosilica-based consolidant applied in the laboratory and *in situ* formed a (~5–10 μm) compact layer made up of silica nanoparticles (Fig. 4a and b), consistent with the size claimed by the manufacturer of the product (i.e., 10–20 nm). FESEM images revealed discontinuities between substrate and consolidant layer (Fig. 4a arrow) as well as crack formation, likely due to the shrinking of the silica gel film upon drying (Fig. 4b). Discontinuities between consolidant and substrate were also detected in the case of earth mock-ups and the rammed earth wall treated with ethyl silicate (Fig. 4c). Crack formation and detachment have been reported previously in the case of nanosilica and ethyl silicate applied to various porous substrates [37]. In mock-ups treated with 2 M KOH solution, the presence of an amorphous phase, showing typical drying cracks of a gel-phase, was observed (Fig. 4d), suggesting that the treatment was successful in inducing mineral dissolution and formation of a cementing phase. We could not, however, unambiguous

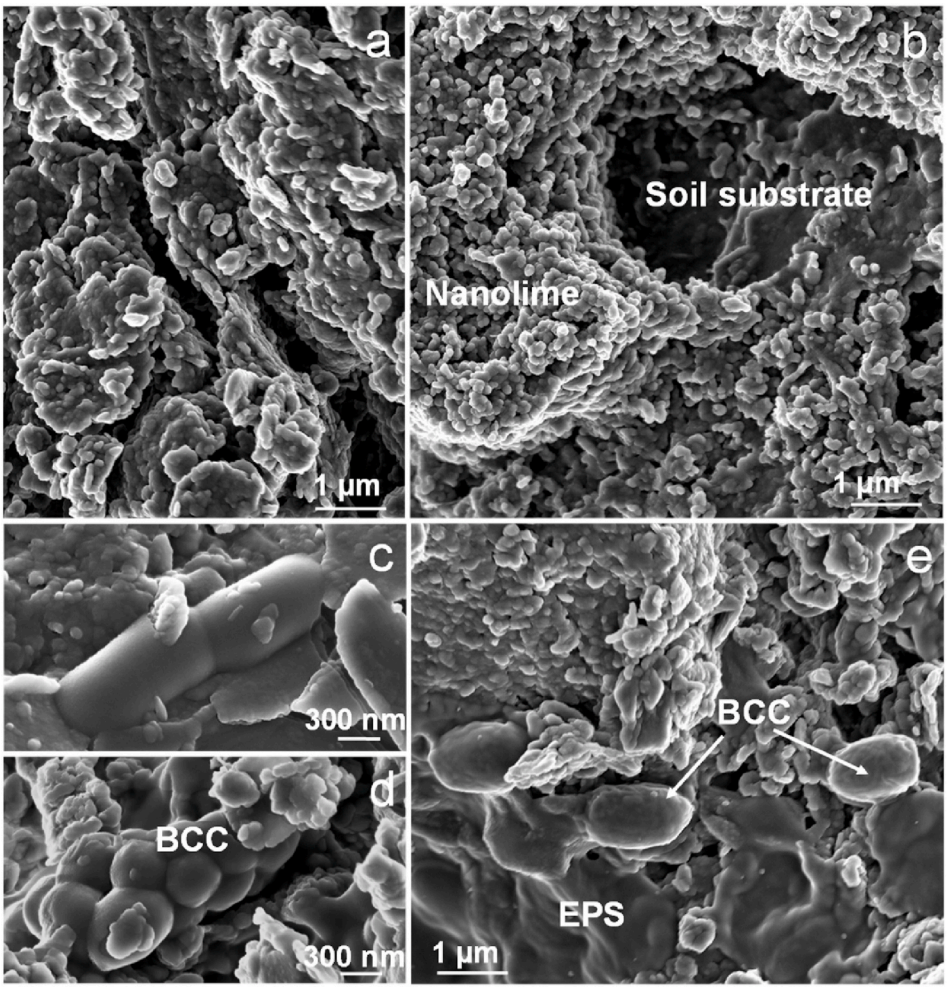

Fig. 3. FESEM images of rammed earth before consolidation (a), after application of nanolime now converted into $CaCO_3$ (b), and upon biomineralization treatment, showing bacterial fission (c) as well as newly-formed bacterial calcium carbonate (BCC) cement covered by EPS (d and e).

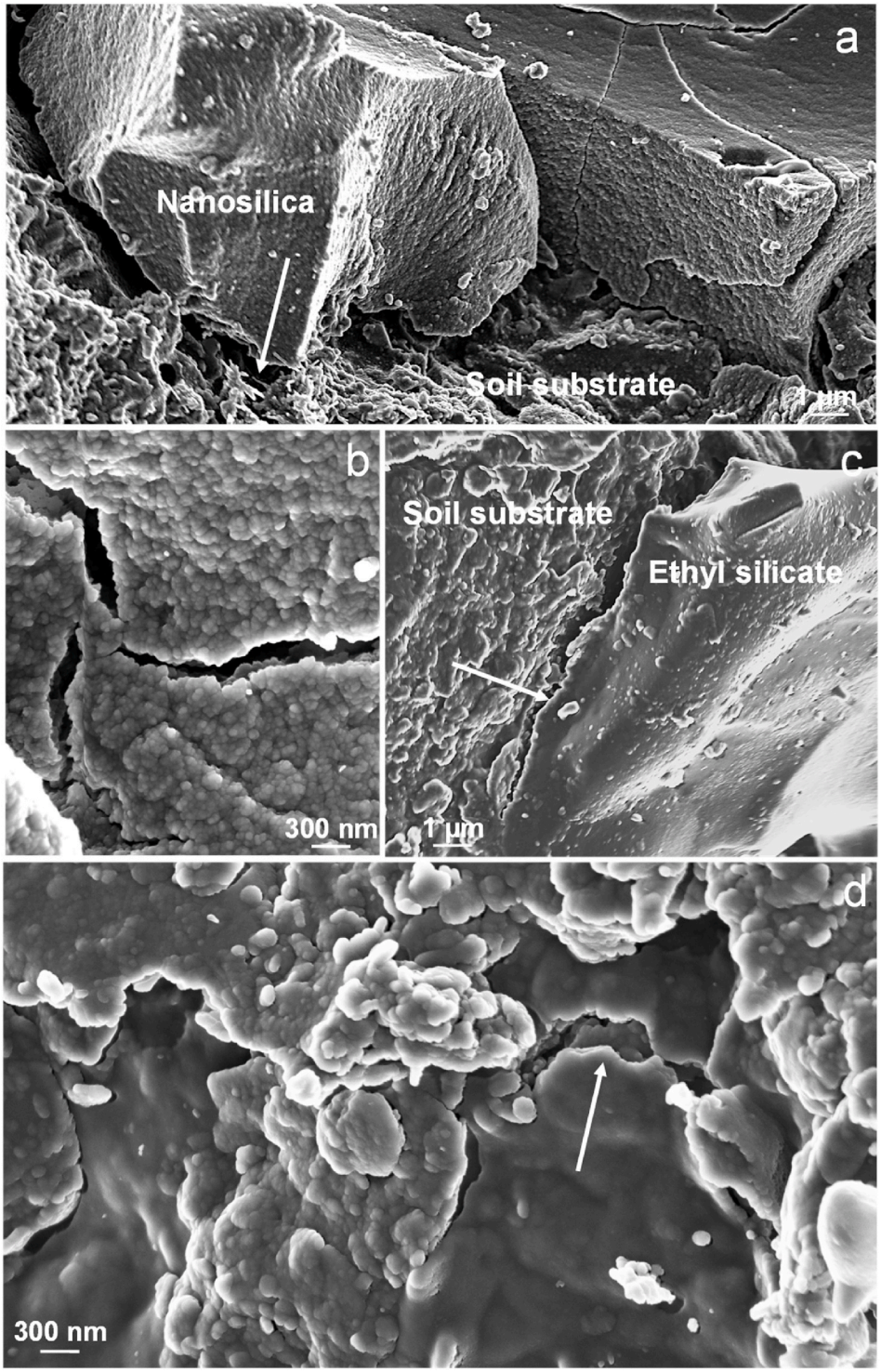

Fig. 4. FESEM images of rammed earth consolidated with nanosilica, showing discontinuity (arrow) between consolidant and substrate (a) and crack formation (b), as well as earth mock-ups consolidated with ethyl silicate showing discontinuity (arrow) between consolidant and substrate (c) and alkaline activation (d), showing gel-phase with crack formation (arrow).

identify such a gel-phase in the rammed earth wall treated with KOH solution.

3.5. Color changes after treatment application

Color change is an important aspect to be considered in the evaluation of consolidation treatments. In the case of laboratory-treated earth mock-ups (Table 3), alkaline activation and biomineralization only caused small color changes (ΔE^* ~3 units), not likely perceivable by the human eye [38]. The color change induced by nanosilica was slightly larger, but below the acceptable limit for conservation treatments (i.e., $\Delta E^* \leq 5$ units [39]). However, this consolidant caused a slight gloss, being the only treatment that led to a small difference (i.e., 0.8 ± 0.3 units) in SCI (specular component included) and SCE (specular component excluded, only considering diffuse reflection) values as compared to the remaining treatments, where the difference never exceeded 0.1 ± 0.1 units (i.e., being within experimental error). Ethyl silicate provoked a significant decrease in luminosity (i.e., darkening of the surface) and consequently caused a considerable color change above the acceptable limit [39]. The most dramatic change, however, was induced by the nanolime treatment, confirming visual observations and FESEM results, which revealed massive surface precipitation of calcite crystals causing a whitish veil on the reddish earth surface. Lanzon et al. [4] reported a similar discoloration in the case of adobe treated with diluted nanolime dispersions.

In the case of the *in situ* treatment, color measurements showed relatively large variations as a result of the significant inhomogeneity of the lime-amended earthen surface (Table 3). All treatments, with the exception of the biomineralization treatment, caused changes above the permissible limit, generally related to an increase in luminosity, especially nanolime- and nanosilica-treated areas showing a dense whitish veil (Fig. 5a and b). In the case of the latter, microscopic observations evidenced massive cracking of the consolidant layer due to rapid drying during the *in situ* treatment at low RH (Fig. S5, Supplementary Information). These cracks cause diffuse light scattering and the treated surface appears white. The alkaline activation treatment induced an important change in the visual perception of the lime-rich areas of the earthen wall (Fig. 5c), which were originally covered by a dark biofilm. Apparently, the high pH of the alkaline solution had a biocidal (bleaching) effect and resulted in the removal of the dark film.

3.6. Water behavior after consolidation treatment of earth mock-ups

Water immersion tests of earth mock-ups revealed drastic differences among the various consolidation treatments regarding their protective action against material loss (Fig. 6). Ethyl silicate was the most effective consolidant and treated samples did not experience any weight loss, even after prolonged immersion for up to 1 month (result not included in the graph). The calculated water absorption rate was 4.5 ± 0.2 wt%/day, which is much lower than that specified for high quality bricks (i.e., 15 wt%/day [40]). The extremely low absorption rate suggests that hydrolysis of ethyl silicate was still not complete after 2 months of curing and conferred a high degree of hydrophobicity to the earth mock-ups. The latter is consistent with the detected alcohol smell of the ethyl silicate-treated samples after 2 months storage. Biomineralization and alkaline activation substantially reduced material loss during the first 15–20 min as compared with the untreated control, while nanolime and nanosilica showed little effectiveness. Test results revealed that the latter two treatments only consolidated a superficially layer of <1 mm in thickness and a protective action was only observed during the first 5 min of immersion (Fig. 6, arrows). Weathering tests performed by Garcia-Vera et al. [41] gave similar results, showing no reduction in erosion rates of earthen plasters treated with diluted nanolime (5 g/L). In an effort to improve the penetration of both consolidants, a second set of samples was treated with diluted suspensions of nanolime (12.5 g/L) and nanosilica (15 wt% solid content). However, these samples showed an identical behavior upon immersion in water as the first set of samples treated with the undiluted consolidants. These results are in agreement with findings by Borsoi et al. [37], who reported very limited penetration (0.5–1 mm) in the case of diluted nanosilica suspension applied to lime mortar.

Static contact angle measurements of untreated and treated earth mock-ups (Table 4) revealed only moderate changes in contact angle and none of the treatments rendered the earth surface hydrophobic, values being generally in the range typically reported for hydrophilic silicate minerals such as quartz ($0^\circ < \Phi < 40^\circ$) [42]. This finding suggests that even though the bulk material of ethyl silicate-consolidated mock-ups showed a high degree of hydrophobicity after 2 months (see above), some hydrolysis of alkoxide groups had taken place at the surface, rendering it hydrophilic. Nanolime caused the largest increase (>200%) in contact angle, the average value being close to that reported for calcite (i.e., 42° [43]). The wettability of the earth surface did not change significantly in the majority of treatments, and the 4 μL drops were absorbed within 2.6–6.1 s by untreated and treated samples. Only the ethyl silicate-

Table 3
Colorimetric coordinates and color change induced by consolidation treatments in the laboratory (mock-ups) and *in situ* (rammed earth wall).

	Sample	L^* (Std. Dev.)	a^* (Std. Dev.)	b^* (Std. Dev.)	ΔE^* (Std. Dev.)
Laboratory	Untreated	49.57 (±1.74)	11.82 (±1.74)	22.79 (±1.74)	–
	Alkaline Act.	50.01 (±1.25)	12.19 (±0.17)	23.55 (±0.33)	1.55 (±0.35)
	Biomineral.	46.67 (±0.97)	12.45 (±0.24)	23.02 (±0.38)	3.21 (±0.97)
	Nanosilica	45.62 (±1.50)	11.84 (±0.37)	21.70 (±0.88)	4.24 (±1.58)
	Ethyl silicate	41.91 (±0.54)	12.31 (±0.20)	20.35 (±0.46)	8.06 (±0.61)
	Nanolime	63.06 (±2.49)	4.75 (±0.76)	−1.53 (±1.70)	28.74 (±2.77)
in situ	Untreated	46.88 (±2.07)	14.20 (±1.27)	21.53 (±1.68)	–
	Alkaline Act.	53.79 (±2.60)	12.33 (±0.61)	20.20 (±0.66)	7.57 (±2.24)
	Biomineral.	45.15 (±1.61)	15.68 (±0.74)	22.00 (±0.56)	2.38 (±1.55)
	Nanosilca	54.75 (±2.34)	10.23 (±0.99)	15.05 (±1.79)	28.93 (±11.99)
	Ethyl silicate	47.86 (±3.25)	11.72 (±1.35)	19.98 (±1.67)	7.14 (±4.69)
	Nanolime	57.91 (±3.64)	10.19 (±0.42)	13.06 (±0.74)	35.99 (±5.50)

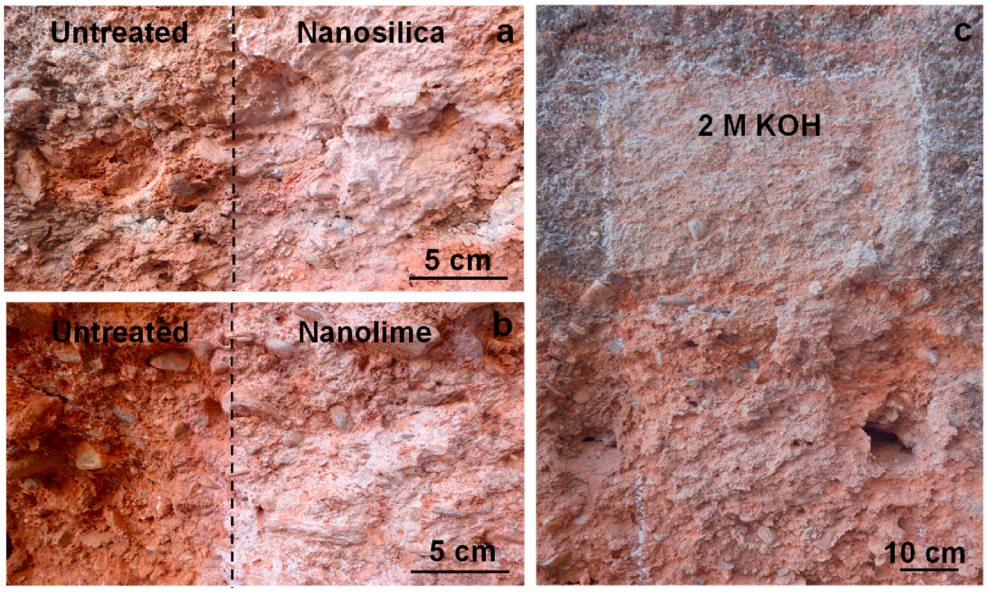

Fig. 5. In situ treatment at the Alhambra Fortress, showing areas consolidated with (a) nanosilica, (b) nanolime, and (c) 2 M KOH solution (alkaline activation).

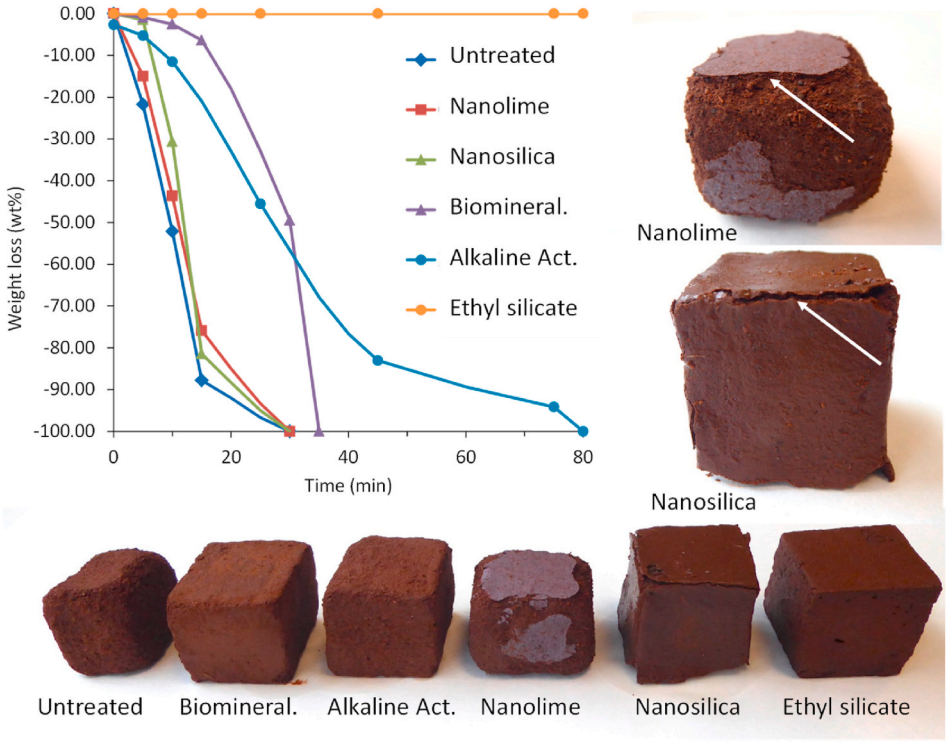

Fig. 6. Weight loss (wt%) of earth mock-ups (4 × 4 × 4 cm) upon immersion in water for different periods of time and aspect of mock-ups after 5 min of immersion, showing a thin consolidated surface layer (arrows) in the case of nanosilica (~600 μm thickness) and nanolime treatments (~200 μm thickness).

and lime-based consolidants delayed water drop absorption substantially, which now took 29.7 and 84.3 s, respectively. In the case of the former this delay was likely related to the reduction in porosity (see below), whereas in the case of the latter, the thin layer of calcium carbonate covering the earth surface rendered the surface slightly less hydrophilic as indicated by the observed increase in contact angle.

Generally, WVTR values were not greatly affected by the majority of consolidation treatments (Table 4) and most variations are likely due to small imperfections caused by the artisanal fabrication of the mock-ups. Only ethyl silicate-treated earth mock-ups

Table 4
Contact angle, absorption time of a 4 μL water drop deposited on the earth surface, water vapor transmission rate (WVTR) of mock-ups, and porosity of mock-ups and rammed earth samples before (untreated) and after consolidation (standard deviation included).

Sample	Contact angle (°)	Absorp. of H_2O drop (s)	WVTR ($g/m^2/day$)	Porosity (%) (mock-ups)	(wall)
Untreated	11.2 ± 1.0	2.6 ± 0.2	177.1 ± 9.3	26.6 ± 0.6	33.9 ± 3.7
Ethyl silicate	24.6 ± 2.4	84.3 ± 11.6	116.7 ± 0.8	20.7 ± 0.8	31.7 ± 2.8
Alkaline Act.	19.8 ± 5.1	5.6 ± 0.5	157.6 ± 14.2	26.9 ± 0.7	34.0 ± 8.5
Biomineral.	16.7 ± 0.4	3.3 ± 1.0	161.7 ± 3.1	24.8 ± 0.7	33.5 ± 6.6
Nanolime	36.6 ± 4.4	29.7 ± 3.7	173.6 ± 5.6	25.6 ± 0.7	35.8 ± 6.2
Nanosilica	22.2 ± 4.5	6.1 ± 1.3	192.1 ± 3.3	25.4 ± 0.7	35.4 ± 8.8

showed a drastic reduction in WVTR of 35%, consistent with a reduction in porosity and a shift in pore size distribution (PSD) (see below).

3.7. Porosity before and after laboratory and in situ consolidation treatment

The total porosity of the untreated earth mock-ups and the rammed earth wall samples was within the range (i.e., 25–45%) typically reported for comparable substrates [44–46]. Porosity measurements also provided important information regarding the consolidation-induced changes, which affected the water (hydric and hygric) behavior of treated substrates. All untreated and treated mock-ups showed a unimodal PSD with a maximum at 2.2–2.4 μm pore diameter. About 55–68% of the total pore volume corresponded to pores with a diameter between 1 and 4 μm and 5.6–7.8% to pores with a diameter >4 μm. With the exception of ethyl silicate, all consolidation treatments caused only minor changes in PSD and total porosity, which were within error and did not influence the water vapor permeability of the mock-ups significantly. This is not surprising in the case of nanolime- and nanosilica-based consolidants as they only consolidated a very thin superficial layer of <1 mm in thickness and hardly affected the pore system of the bulk material. The biomineralization treatment reduced the volume of pores with a diameter ≤0.1 μm by 50%, but, as indicated above, only caused minor changes in the hygric behavior. Ethyl silicate filled an important amount of capillary pores, leading to a 27% reduction in the volume of pores with a diameter ≤1 μm and a 22% reduction in total porosity. Consequently, connectivity of the pore system was reduced, which explains the decrease in WVTR by more than 30% and the significantly slower absorption of water drops (Table 4).

The total porosity of rammed earth wall samples was on average ~20% higher than that of earth mock-ups and showed important variations depending on the state of degradation, which made the detection of any significant changes upon consolidation very difficult (Table 4). Two pore populations were identified in untreated rammed earth samples (Fig. 7b). One population with pores between 4 and 300 μm in diameter showing several maxima with an important contribution of macro- and megapores possibly due to fracturing, and a second population with pores of <4 μm in diameter. Ethyl silicate was the only consolidant that induced a slight decrease of 5% in total porosity; however, such a value was within error. PSD curves of rammed earth treated with either ethyl silicate or nanosilica revealed a reduction in the volume of pores <4 μm in diameter and an additional maximum at 0.006 μm in diameter, corresponding to gel pores in the newly formed silica gel [47]. The nanolime treatment, in contrast, seemed to have reduced the volume of pores >30 μm in diameter and PDS curves showed an additional maximum at 0.1 μm in diameter, possibly related to pores within the nanostructured $CaCO_3$ formed upon carbonation. The remaining consolidants did not modify the porosity and PSD significantly, and are thus not shown in Fig. 7b.

3.8. Changes in mechanical strength after treatment

Compressive strength (Table 5) of untreated earth mock-ups was below standard specifications for earthen building materials (i.e., 1.18–2.07 MPa [48]). The majority of consolidation treatments did not affect the samples' compressive strength or drilling resistance

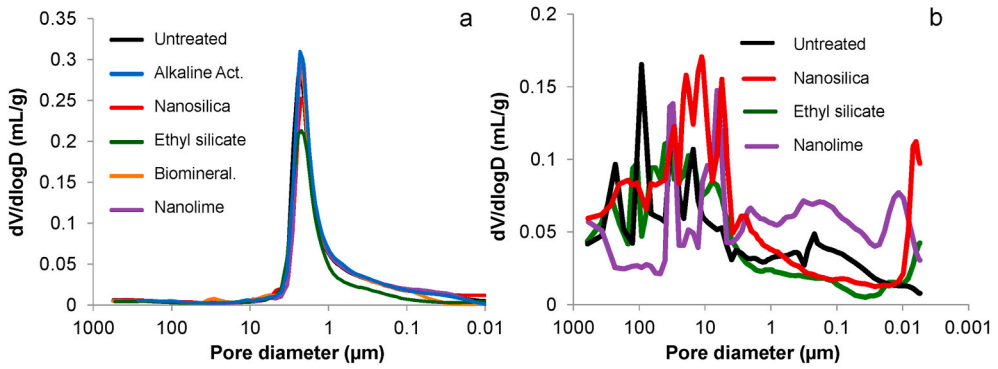

Fig. 7. Log differential intrusion versus pore diameter (μm) of representative earth mock-ups (a) and rammed earth (b) samples before and after treatment with various consolidants.

Table 5
Compressive strength and drilling resistance (DR) measurements of mock-ups and the rammed earth wall before and after consolidation (standard deviation included).

Sample	Compress. Strength (MPa) (mock-ups)		Drill. depth (mm)	DR (N) (mock-ups)	DR (N) (wall)
Untreated	1.00 ± 0.22	0–20	0.87 ± 0.44	1.71 ± 1.40	
Nanolime	1.02 ± 0.11	0–20	1.11 ± 0.55	2.65 ± 1.79	
Nanosilica	1.04 ± 0.18	0–0.6	2.70 ± 0.43	2.53 ± 1.93	
		0.7–20	1.00 ± 0.25	2.53 ± 1.93	
Biomineral.	1.23 ± 0.10	0–20	1.00 ± 0.44	1.61 ± 1.36	
Alkaline Act.	1.30 ± 0.11	0–20	1.26 ± 0.58	2.18 ± 1.78	
Ethyl silicate	3.54 ± 0.13	0–6.5	12.16 ± 2.63	2.87 ± 1.73	
		6.6–20	6.54 ± 0.54	2.87 ± 1.73	

(DR) significantly and changes observed were in most cases within error. Only ethyl silicate induced a drastic increase in compressive strength (>300%) and in DR of earth mock-ups (Table 5). This increase in strength was especially evident up to 6.5 mm depth as shown by DR measurements (Table 5, Fig. 8). This testing method also confirmed prior observations regarding the formation of a thin surface layer with increased strength in the case of nanosilica-treated mock-ups, revealing a noticeable increase in strength over the first 0.6 mm (Table 5). As a result of the significant inhomogeneity of the rammed earth wall, characterized by the presence of coarse particles (i.e., silicate rocks/pebbles such as quartzite and schist) and large voids often due to delamination and scaling, it was very difficult to obtain reliable DR results *in situ*. In the analysis of the acquired DR data of untreated and treated rammed earth wall, spikes due to larger hard mineral grains were not considered in order to establish a more accurate quantification of the possible strengthening effect on the clay-rich matrix. However, the DR results presented here should rather be considered as a trend than as absolute values. Considering the high standard deviation, none of the consolidation treatments induced significant changes in the mechanical strength and small differences in strength might be substrate-related. Remarkably, ethyl silicate did not show the same effectiveness as observed in the laboratory-treated mock-ups, likely because the consolidant was unable to fill larger voids as indicated by porosity measurements, which remained basically unchanged upon treatment in the case of the rammed earth wall (Table 4).

The peeling test of laboratory-treated mock-ups showed important differences among the various consolidants (Table 6). Ethyl silicate, nanosilica and nanolime improved surface cohesion significantly. Lanzon et al. [4] reported similar findings in the case of adobe treated with nanolime, which reduced the amount of material removed by adhesive strips by 60%. Alkaline activation and biomineralization treatments, in contrast, did not increase surface cohesion. Visual observations revealed an increase in surface roughness in the case of earth mock-ups treated with the latter two consolidants, likely being the result of superficial erosion induced by the application of these water-based consolidants.

Peeling tape test results at the Alhambra fortress (Table 6) showed large variations due to the significant inhomogeneity and surface roughness of the severely eroded rammed earth surface. Indeed, the advanced state of deterioration led to weight losses, which were up to two orders of magnitude higher than those of laboratory-treated mock-ups. Most consolidants induced only minor improvements considering the large standard deviation. However, nanosilica improved the surface cohesion drastically, whereas the alkaline activation, as in the case of the earth mock-ups, might have even worsened surface cohesion slightly.

4. Discussion

Test results not only revealed significant differences in performance among the various consolidants, but also important limitations regarding their *in situ* evaluation as it has also been described in the case of stone consolidation treatments [7]. Compared to many other building materials, rammed earth is characterized by its often extreme inhomogeneity (i.e., compositional and textural

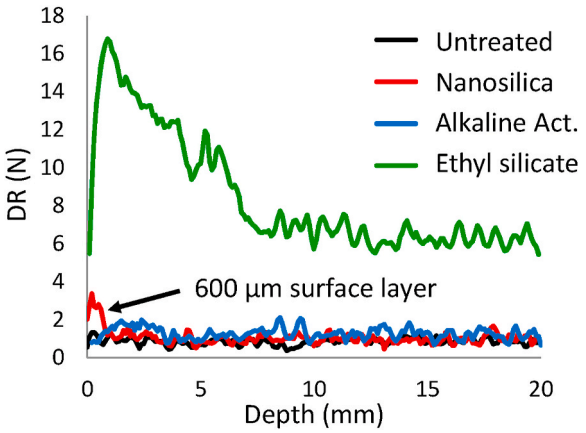

Fig. 8. Representative drilling resistance profiles of selected mock-ups treated in the laboratory.

Table 6
Peeling test results (weight loss, g/m^2) of earth mock-ups and rammed earth wall before and after consolidation.

Sample	Mock-ups (laboratory)	Rammed earth wall (*in situ*)
Untreated	9.9 ± 2.5	139.0 ± 59.8
Ethyl silicate	1.0 ± 1.2	101.1 ± 40.9
Nanosilica	3.7 ± 0.6	5.7 ± 5.0
Nanolime	4.7 ± 1.8	116.2 ± 79.2
Biomineralization	13.5 ± 2.3	115.4 ± 63.3
Alkaline Activation	25.0 ± 14.0	146.9 ± 106.0

variations) caused by the presence of large pebbles and certain deterioration phenomena such as scaling. In the case of lime-amended lime, inhomogeneity is further exacerbated as a result of substantial differences in mechanical strength between clay- and lime-rich layers. Consequently, it was very difficult to obtain conclusive results with *in situ* evaluation methods such as drilling resistance or peeling tape test measurements. The assessment was further complicated by the extreme roughness and low cohesion of the surface, which excluded other common *in situ* test procedures such as ultrasonic velocity measurements or the Karsten tube test. Thus, laboratory studies were essential to obtain an insight into the performance of the different consolidants, even though, questions might arise regarding the transferability of these results due to differences in substrate properties, and environmental conditions during consolidant application [7]. To this regard the state of conservation of the earthen substrate has also to be considered, as degradation can induce important compositional and textural changes.

Ethyl silicate, the most widely used consolidant for earthen structures since its first application in the late 1960s [1], had the biggest impact on the weathering resistance of laboratory-treated mock-ups. Even though induced color changes were above the established limit, its apparent effectiveness might make it the consolidant of choice. However, laboratory results showed that hydrolysis of ethyl silicate was not complete after 2 months and that the improved weathering resistance was achieved at the expense of important modifications of the pore system that limited water vapor transport and drastically increased compressive strength and drilling resistance. These changes can lead to a significant difference in the physical-mechanical behavior between the consolidated outer layer and the unconsolidated core and might cause scaling. *In situ* results did not confirm these findings and only minor changes in mechanical strength and porosity were observed upon treatment. This suggests that the impact of ethyl silicate greatly depends on the substrate's pore system, which in turn is influenced by the degree of degradation of the earthen structure. Chiari [49] stated that ethyl silicate would not act as glue and Wheeler [13] pointed out that consolidation of porous substrates with pores >50 μm would not be feasible. These assertions are in line with our findings, showing no changes in the volume of pores >4 μm of the severely eroded rammed earth wall. Although ethyl silicate improved surface cohesion to a certain extent, FESEM images revealed discontinuities between the soil substrate and the consolidant layer and XRD results suggest that clay swelling might not completely be prevented. These findings question the long-term effectiveness of ethyl silicate-based consolidants for earthen structures. This is an issue that has been raised previously in relation to clay-rich substrates, which undergo expansion and contraction due to changes in moisture content [9,50]. Some experimental results even suggest that ethyl silicate could be responsible for an increase in clay swelling [13,51]. Additional laboratory and field studies are advised to determine the treatments long-term effectiveness in the case of clay-rich substrates.

Alkaline activation using 2 M KOH solution had only a limited effect on the substrate's mechanical strength, but improved its weathering resistance. This was likely due to the formation of a gel-phase upon clay dissolution, which acted as a cementing agent, even though the water-based consolidant seemed to have impacted surface cohesion negatively as revealed by peeling test results. Previous studies involving KOH solution of higher concentration (5 M KOH), demonstrated higher efficacy regarding weathering and strength improvements in earthen materials as compared to laboratory- and *in situ*-treated samples of this study, suggesting that a correct dosing is of outmost importance [9,11]. In this respect, the application conditions have also to be considered. Indeed, the high RH (~80%) maintained during application to facilitate dissolution-precipitation reactions impeded substrate drying and substantially limited consolidant absorption under laboratory conditions, causing clay swelling and pore clogging in the water saturated substrate. It seems advisable to maintain a moderate RH (50–60%) during consolidant application to guarantee adequate absorption, and increase the RH during the subsequent curing process to promote clay dissolution and precipitation of cementitious phases. In the case of the *in situ* treatment, the short curing period (i.e., 7 days) at relatively low RH was likely responsible for the limited treatment effectiveness. Additional water spraying and plastic covering could be used to maintain a sufficiently high moisture content during curing, which should last at least three weeks. A previous study [9] has shown that further increase in strength can be expected over time as unreacted KOH continues to react as the substrate's moisture content increases (during the rainy season) and generates additional cementing phases. *In situ* observations at the Alhambra revealed that the alkaline activation treatment induced a noticeable color change, especially in areas which were covered by a dark biofilm. On occasions the biocidal effect of the alkaline KOH solution might suppose a positive side effect, making additional biocide treatments unnecessary. However, tests should be performed prior to any applications to avoid any undesired visual impact.

The quantification of carbonatogenic bacteria proved the effectiveness of the biomineralization treatment involving the application of a sterile nutritive solution, both, in the laboratory and *in situ*. Importantly, despite increased bacterial activity, no significant color changes could be detected. Even though mechanical strength did not increase, laboratory results clearly showed an improvement of the water resistance, as indicated by a significant reduction in material loss during water immersion, while WVTR and PSD remained basically unaltered. Improved water resistance is likely related to the generation of bacterial calcium carbonate cement and bacterially-derived EPS evidenced by FESEM, which promoted the cementation of clay particles and the formation of a protective

biofilm upon laboratory and *in situ* treatment. Nonetheless, the treatment's impact on the clays' swelling capacity was limited according to XRD and clear evidence for the intercalation of EPS into the interlayer space of expansive clay minerals that could reduce clay swelling as observed in the case of tuff stone at the Maya site of Copan [21] was not obtained. Better results might be obtained by prolonging the treatment duration or increasing *T* during treatment. Note that findings by Sun et al. [52] showed that at 30 °C calcium carbonate precipitation rates of carbonatogenic bacteria (e.g. Bacillus megaterium) increased considerably over time, while they did not differ significantly in the 15–25 °C *T* range. In any case, alternative biomineralization treatments should also be explored to identify more effective strategies. Pathways based on the application of either a self-inoculation method using indigenous carbonatogenic bacteria capable of oxidative deamination of amino acids [16] or cultured ureolytic bacteria [53–55] seem viable candidates for the consolidation of earthen structures. The former have successfully been applied for the consolidation of heavily degraded limestone, while the latter have been used for the self-healing of concrete and the cementation of soil as they are able to produce high amounts of carbonate within a short period of time [56]. Future studies should also focus on treatment-induced structural changes in clay minerals and verify whether a long-lasting reduction in the soil's swelling capacity can be achieved.

Nanolime and nanosilica treatments provoked a considerable color change of the reddish earthen substrate, with no improvement in weathering resistance or mechanical strength other than an increase in cohesion of an extremely thin surface layer. These effects where observed both in the laboratory and *in situ*. According to XRD analysis, both consolidants reduced clay swelling to a certain extent. However, it has to be kept in mind that they only consolidated the outermost surface layer and had no effect on the bulk material, potentially generating damage due to scaling of the consolidated layer. DR measurement and water immersion tests confirmed the limited penetration (<1 mm) of both consolidants. In the case of nanosilica, penetration might be hindered as a result of clay swelling induced by the water-based consolidant, which can cause a reduction in pore size and total porosity. Limited penetration in the case of nanolime might be in part due to back migration during solvent evaporation. However, particle-substrate interactions could also contribute to the problem. Camerini et al. [5] have shown that the attractive forces between silica and $Ca(OH)_2$ nanoparticles, having opposite surface charge, caused flocculation and the formation of aggregates of up to 1 μm in size. Considering the high content in silicate minerals in earthen materials, similar interactions could be at play, leading to clogging of capillary pores and preventing adequate penetration. Presumably, the use of long-chain alcohols with higher vapor pressure (and lower evaporation rates) could reduce back migration and might better shield nanolime particles by creating an external layer of alkyl chains following their adsorption, which can promote steric repulsion ultimately preventing the formation of aggregates and facilitating penetration [57].

Overall, these results confirm previous findings [9,11], indicating that consolidant penetration is one of the most important parameters for a successful consolidation of earthen materials. Indeed, Chiari's [49] recommendation regarding a minimum penetration depth of at least 1–2 cm for earthen materials is in agreement with our observations. Furthermore, it has been shown that water-based solutions (e.g. alkaline KOH solution) were able to penetrate earthen substrates quite well and consolidated a ~2 cm thick layer [9,11]. Likely, the high K^+ concentration of the alkaline solution counteracted clay swelling at least in part, thus enabling sufficient penetration [14]. The same effect is to be expected for the water-based nutritional solution used for bacterial biomineralization, which contains Ca^{2+}. It is therefore probable that bacterial biomineralization also occurs at a significant depth and not only at the surface of the earthen wall.

5. Concluding remarks

Results of laboratory and *in situ* analyses and tests have shown that the consolidation of earthen architecture is complicated by material-related aspects, which determine consolidant-substrate interactions. The conventional ethyl silicate-based consolidant had the biggest impact on mechanical strength and weathering resistance in laboratory tests, but its *in situ* performance was limited. Depending on pore size distribution, this consolidant can significantly modify the substrate's water transport. Furthermore, its long-term effectiveness might be limited as clay swelling is not completely prevented by the treatment, while a consolidated layer with a very different physical-mechanical behavior from the bulk material is created. The remaining consolidants had only limited or no impact on the substrate strength. Nanolime and nanosilica showed very limited penetration and only improved the cohesion of the outermost surface layer, but did not increase water resistance of the bulk material. Consequently, their use might be limited to substrates with powdery surface. Alkaline activation and biomineralization treatments, in contrast, improved the weathering resistance. However, modifications to current application protocols of these novel consolidation treatments seem necessary to optimize their efficacy when applied *in situ*. Laboratory tests should be performed to evaluate the feasibility of alternative biomineralization strategies involving the self-inoculation of activated indigenous bacteria or application of cultured ureolytic bacteria. Additional nanoscale studies are required to investigate the possible positive effect of intercalated bacterial-derived exopolymeric substances, as well as the long-term impact of ethyl silicate, on the swelling behavior of the clay-rich earthen substrate. It would also be essential to unambiguously determine whether charge-related interactions between nanolime particles and silicate-rich substrates are, at least in part, responsible for the observed limited consolidant penetration and whether the use of long-chain alcohols with lower vapor pressure would promote steric repulsion and limit back migration and thus improve penetration.

Finally, our results proved that the *in situ* evaluation of the consolidants' efficacy was very challenging due to the extreme inhomogeneity of the earthen material commonly encountered, making laboratory studies indispensable as part of a comprehensive evaluation that complement field assessment.

Funding

This research was financed by the Unidad de Excelencia "UCE2018-01 - Ciencia en la Alhambra" (UGR), Unidad Cientifica de Excelencia "UCE.PP2016.05" (UGR), and the Research Group "RNM0179" (Junta de Andalucia).

Credit authorship contribution statement

KE: conceptualization, laboratory and field testing, data analysis, writing and editing with input of all authors; ECG and CRN: field testing; FJ: microbiological analysis. CBR: mechanical testing.

Declaration of competing interest

The authors declare that they have no known competing financial interests or personal relationships that could have appeared to influence the work reported in this paper.

Acknowledgement

This research is part of the collaboration between the Patronato de la Alhambra y Generalife (Granada, Spain), the Getty Conservation Institute (Los Angeles, USA), and the University of Granada (Spain). We thank KBYO BIOLOGICAL S.L. (Spain) for supplying the patented nutritive solution M − 3P and R. Rubio Domene, J. Otero, as well as M. Burgos Ruiz for their help with *in situ* consolidation. We also thank C. Cardell, M.T. González Muñoz, J.M. Azañón Hernández, and A. Leslie for their support and advice. Funding for open access charge: Universidad de Granada / CBUA.

Appendix A. Supplementary data

Supplementary data to this article can be found online at https://doi.org/10.1016/j.jobe.2022.104081.

References

[1] G. Torraca, G. Chiari, G. Gullini, Report on mud brick preservation, Mesopotamia 7 (1972) 259–286.
[2] K. Elert, E. Sebastián, I. Valverde, C. Rodriguez-Navarro, Alkaline treatment of clay minerals from the Alhambra Formation: implications for the conservation of earthen architecture, Appl. Clay Sci. 39 (2008) 122–132.
[3] A. Oliver, Conservation of nondecorated earthen materials, in: E. Avrami, H. Guillaud, M. Hardy (Eds.), Terra Literature Review, Getty Conservation Institute, Los Angeles, 2008, pp. 108–123.
[4] M. Lanzón, J.A. Madrid, A. Martínez-Arredondo, S. Mónaco, Use of diluted $Ca(OH)_2$ suspensions and their transformation into nanostructured $CaCO_3$ coatings: a case study in strengthening heritage materials (stucco, adobe and stone), Appl. Surf. Sci. 424 (2017) 20–27.
[5] R. Camerini, D. Chelazzi, R. Giorgi, P. Baglioni, Hybrid nano-composites for the consolidation of earthen masonry, J. Colloid Interface Sci. 539 (2019) 504–515.
[6] F. Pacheco-Torgal, J. Said, Earth construction: lessons from the past for future eco-efficient construction, Construct. Build. Mater. 29 (2012) 512–519.
[7] Y. Praticò, F. Caruso, J. Delgado Rodrigues, F. Girardet, E. Sassoni, G.W. Scherer, V. Vergès-Belmin, N.R. Weiss, G. Wheeler, R.J. Flatt, Stone consolidation: a critical discussion of theoretical insights and field practice, RILEM Tech. Lett. 4 (2020) 145–153.
[8] F.T. Madsen, M. Müller-Vonmoos, The swelling behaviour of clays, Appl. Clay Sci. 4 (1989) 143–156.
[9] K. Elert, P. Bel-Anzué, L. Monasterio-Guillot, E. Sebastián Pardo, Performance of alkaline activation for the consolidation of earthen architecture, J. Cult. Herit. 39 (2019) 93–102.
[10] E. Doehne, C.A. Price, Stone Conservation: an Overview of Current Research, Getty Conservation Institute, Los Angeles, 2010.
[11] K. Elert, E. Sebastían Pardo, C. Rodriguez-Navarro, Alkaline activation as an alternative method for the consolidation of earthen architecture, J. Cult. Herit. 16 (2015) 461–469.
[12] K. Elert, E. Ruiz Agudo, C. Cardell, A. Leslie, D. Gulotta, F. Jroundi, C. Jiménez López, M.T. González Muñoz, J.M. Azañón, M.R. Blanc García, M.P. Sáez Pérez, E. Correa, C. Rodríguez–Navarro, Bacterial consolidation of earthen structures: preliminary results at the Alhambra fortress (Granada, Spain), in: L. Rainer, L. Meyer, F. Matero, L.F. Guerrero Baca (Eds.), Proceedings of the Terra 2022 - 13th World Congress on Earthen Architectural Heritage, Getty Conservation Institute, Los Angeles, 2022.
[13] G. Wheeler, Alkoxysilanes and the Consolidation of Stone, Getty Conservation Institute, Los Angeles, 2005.
[14] O. Karnland, S. Olsson, U. Nilsson, P. Sellin, Experimentally determined swelling pressures and geochemical interactions of compacted Wyoming bentonite with highly alkaline solutions, Phys. Chem. Earth 32 (2007) 275–286.
[15] R.L. Anderson, I. Ratcliffe, H.C. Greenwell, P.A. Williams, S. Cliffe, P.V. Coveney, Clay swelling—a challenge in the oilfield, Earth Sci. Rev. 98 (2010) 201–216.
[16] F. Jroundi, M. Schiro, E. Ruiz-Agudo, K. Elert, I. Martín-Sánchez, M.T. González-Muñoz, C. Rodriguez-Navarro, Protection and consolidation of stone heritage by self-inoculation with indigenous carbonatogenic bacterial communities, Nat. Commun. 8 (2017) 1–13.
[17] A. Alimova, A. Katz, N. Steiner, E. Rudolph, H. Wei, J.C. Steiner, P. Gottlieb, Bacteria-clay interaction: structural changes in smectite induced during biofilm formation, Clay Clay Miner. 57 (2009) 205–212.
[18] P. Tiano, L. Biagiotti, G. Mastromei, Bacterial bio-mediated calcite precipitation for monumental stones conservation: methods of evaluation, J. Microbiol. Methods 36 (1999) 139–145.
[19] C. Jimenez-Lopez, F. Jroundi, C. Pascolini, C. Rodriguez-Navarro, G. Pinar-Larrubia, M. Rodriguez-Gallego, M.T. González-Muñoz, Consolidation of quarry calcarenite by calcium carbonate precipitation induced by bacteria activated among the microbiota inhabiting the stone, Int. Biodeterior. Biodegrad. 62 (2008) 352–363.
[20] M.T. González-Muñoz, C. Rodriguez-Navarro, C. Jimenez-Lopez, M. Rodriguez-Gallego, Method and Product for Protecting and Reinforcing Construction and Ornamental Materials, 2008 publication number, Spanish patent P200602030 (WO2008009771).
[21] K. Elert, E. Ruiz-Agudo, F. Jroundi, M.T. Gonzalez-Muñoz, B.W. Fash, W.L. Fash, N. Valentine, A. de Tagle, C. Rodriguez-Navarro, Degradation of ancient Maya carved tuff stone at Copan and its bacterial bioconservation, npj Mater, Degra 5 (2021) 1–12.
[22] F. Jroundi, M.T. Gonzalez-Muñoz, A. Garcia-Bueno, C. Rodriguez-Navarro, Consolidation of archaeological gypsum plaster by bacterial biomineralization of calcium carbonate, Acta Biomater. 10 (2014) 3844–3854.
[23] J.D. Martín-Ramos, Using XPowder: A Software Package for Powder X-Ray Diffraction Analysis, 2004, ISBN 84-609-1497-6.
[24] Bureau of Indian Standards, IS 3495:1992 Methods of Tests of Burnt Clay Building Bricks, Part 2, Determination of Water Absorption, New Delhi, 2002.
[25] Y. Luo, P. Zhou, P. Ni, X. Peng, J. Ye, Degradation of rammed earth under soluble salts attack and drying-wetting cycles: the case of Fujian Tulou, China, Appl, Clay Sci. 212 (2021) 106202.
[26] C.T.S. Beckett, P.A. Jaquin, J.C. Morel, Weathering the storm: a framework to assess the resistance of earthen structures to water damage, Construct. Build. Mater. 242 (2020) 118098.
[27] Aenor, Une-EN 828 Adhesivos, Mojabilidad. Determinación por medida del ángulo de contacto y de la tensión superficial crítica de la superficie sólida, 2013. Madrid.

[28] Aenor, Une-EN 15803, Conservation of Cultural Property - Test Methods - Determination of Water Vapour Permeability, dp), Madrid, 2010.
[29] Aenor, Une-EN 1015-11, Methods of Test for Mortar for Masonry. Part 11: Determination of Flexural and Compressive Strength of Hardened Mortar, 2020. Madrid.
[30] M. Drácký, J. Lesák, S. Rescic, Z. Slížková, P. Tiano, J. Valach, Standardization of peeling tests for assessing the cohesion and consolidation characteristics of historic stone surfaces, Mater. Struct. 45 (2012) 505–520.
[31] A. Ito, R. Wagai, Global distribution of clay-size minerals on land surface for biogeochemical and climatological studies, Sci. Data 4 (2017) 1–11.
[32] D.M. Moore, R.C. Reynolds, X-ray Diffraction and the Identification and Analysis of Clay Minerals, Oxford University Press, Oxford, 1989.
[33] D.L. Whitney, B.W. Evans, Abbreviations for names of rock-forming minerals, Am. Mineral. 95 (2010) 185–187.
[34] A.E. Charola, J. Pühringer, M. Steiger, Gypsum: a review of its role in the deterioration of building materials, Environ. Geol. 52 (2007) 339–352.
[35] D.N. Little, S. Nair, B. Herbert, Addressing sulfate-induced heave in lime treated soils, J. Geotech. Geoenviron. Eng. 136 (2010) 110–118.
[36] C. Rodriguez-Navarro, E. Ruiz-Agudo, Nanolimes: from synthesis to application, Pure Appl. Chem. 90 (2018) 523–550.
[37] G. Borsoi, R. Veiga, A. Santos Silva, Effect of nanostructured lime-based and silica-based products on the consolidation of historical renders, in: HMC13: Proceedings of the 3rd Historic Mortars Conference, Glasgow, University of the West of Scotland, Glasgow, 2013, pp. 11–14, 9.2013.
[38] R.S. Berns, Principles of Color Technology, third ed., Wiley-Blackwell, Hoboken, 2000.
[39] H.R. Sasse, R. Snethlage, Methods for the evaluation of stone consolidation treatments, in: N.S. Baer, R. Snethlage (Eds.), Saving Our Architectural Heritage. The Conservation of Historic Stone Structures, John Wiley & Sons Ltd., Chichester, 1997, pp. 223–243.
[40] Bureau of Indian Standards, IS 1077:1992 Common Burnt Clay Building, Bricks - Specification, New Delhi, 2007.
[41] V.E. García-Vera, A.J. Tenza-Abril, A.M. Solak, M. Lanzón, Calcium hydroxide nanoparticles coatings applied on cultural heritage materials: their influence on physical characteristics of earthen plasters, Appl. Surf. Sci. 504 (2020) 144195.
[42] R.N. Lamb, D.N. Furlong, Controlled wettability of quartz surfaces, J. Chem. Soc. Faraday. Trans. 78 (1982) 61–73.
[43] C. Rodriguez-Navarro, E. Doehne, E. Sebastian, Influencing crystallization damage in porous materials through the use of surfactants: experimental results using sodium dodecyl sulfate and cetyldimethylbenzyl-ammonium chloride, Langmuir 16 (2000) 947–954.
[44] P.W. Brown, C.R. Robbins, J.R. Clifton, Adobe II: factors affecting the durability of adobe structures, Stud. Conserv. 24 (1979) 23–39.
[45] S. Ahmadi, Adobe Conservation: Evaluation of Silicone and Acrylic Consolidants, Master Thesis, Queen's University, Kingston, Canada, 2008.
[46] C.H. Kouakou, J.C. Morel, Strength and elasto-plastic properties of non-industrial building materials manufactured with clay as a natural binder, Appl. Clay Sci. 44 (2009) 27–34.
[47] P.J. Davis, C.J. Brinker, D.M. Smith, Pore structure evolution in silica gel during aging/drying I. Temporal and thermal aging, J. Non-Cryst. Solids 142 (1992) 189–196.
[48] D. Silveira, H. Varum, A. Costa, T. Martins, H. Pereira, J. Almeida, Mechanical properties of adobe bricks in ancient constructions, Construct. Build. Mater. 28 (2012) 36–44.
[49] G. Chiari, Characterization of adobe as building material. Preservation techniques, in: Adobe. International Symposium and Training Workshop on the Conservation of Adobe in Lima-Cusco, UNDP/UNESCO, Peru and ICCROM, Rome, 1983, pp. 31–40, 1983.
[50] E. Wendler, D.D. Klemm, R. Snethlage, Consolidation and hydrophobic treatment of natural stone, in: J.M. Baker, H. Davis, A.J. Majumdar, P.J. Nixon (Eds.), Proceedings of the 5th International Conference on Durability of Building Materials and Components, Chapman and Hall, London, 1990, pp. 203–212.
[51] M. Tiennot, A. Liegey, A. Bourges, J.D. Mertz, A. Bouquillon, P. Lehuede, V. Bout, P. Recourt, B. Andre-Salvini, B. Monasse, A. Burr, E. Darque Cerretti, Clays, unbaked earth tablets, and ethyl silicate: towards an understanding of the consolidation mechanisms, in: J. Bridgland (Ed.), Preprints of ICOM-CC 17th Triennial Conference, The International Council of Museums, Paris, 2014, pp. 1–9.
[52] X. Sun, L. Miao, T. Tong, C. Wang, Study of the effect of temperature on microbially induced carbonate precipitation, Acta Geotech 14 (2019) 627–638.
[53] V. Ivanov, J. Chu, Applications of microorganisms to geotechnical engineering for bioclogging and biocementation of soil in situ, Rev. Environ. Sci. Biotechnol. 7 (2008) 139–153.
[54] J. García-González, A.S. Pereira, P.C. Lemos, N. Almeida, V. Silva, A. Candeias, A. Juan-Valdés, P. Faria, Effect of surface biotreatments on construction materials, Construct. Build. Mater. 241 (2020) 118019.
[55] W. De Muynck, N. De Belie, W. Verstraete, Microbial carbonate precipitation in construction materials: a review, Ecol. Eng. 36 (2010) 118–136.
[56] J. Dick, W. De Windt, B. De Graef, H. Saveyn, P. Van der Meeren, N. De Belie, W. Verstraete, Bio-deposition of a calcium carbonate layer on degraded limestone by Bacillus species, Biodegradation 17 (2006) 357–367.
[57] E. Fratini, M.G. Page, R. Giorgi, H. Cölfen, P. Baglioni, B. Demé, T. Zemb, Competitive surface adsorption of solvent molecules and compactness of agglomeration in calcium hydroxide nanoparticles, Langmuir 23 (2007) 2330–2338.